

CHIRAL PERTURBATION THEORY ¹

J. Bijnens ¹, G. Ecker ² and J. Gasser ³

¹) NORDITA, Blegdamsvej 17, DK-2100 Copenhagen

²) Inst. Theor. Physik, Univ. Wien, Boltzmanngasse 5, A-1090 Wien

³) Inst. Theor. Physik, Univ. Bern, Sidlerstrasse 5, CH-3012 Bern

¹To be published in the second edition of the DAΦNE Physics Handbook, eds. L. Maiani, G. Pancheri and N. Paver

1 Prelude

Chiral perturbation theory (CHPT) is a systematic method to analyse the low-energy structure of the Standard Model. In particular, it allows one to determine the low-energy behaviour of the Green functions built from quark currents, like the electromagnetic form factor of the mesons or the meson-meson scattering amplitudes. Matrix elements for semileptonic decays are calculable from quark current correlators as well, because the momenta of the external particles are small with respect to the W mass, and the weak interactions reduce to the current \times current form in this case. For illustration, we note the following correspondence:

$$\langle 0 | T A_\mu^i(x) V_\rho^{em}(y) A_\nu^j(z) | 0 \rangle \quad : \quad \text{electromagnetic form factor}$$

$$\langle 0 | T A_\mu^i(x) A_\nu^k(y) A_\rho^l(z) A_\sigma^m(w) | 0 \rangle \quad : \quad \pi\pi \text{ scattering amplitude}$$

$$\langle 0 | T A_\mu^l(x) \bar{u}(y) \gamma_\nu s(y) A_\rho^m(z) | 0 \rangle \quad : \quad K \rightarrow \pi e \nu \text{ decay} .$$

Here A_μ^i , V_ρ^{em} and Q denote the axial and the electromagnetic current and the charge matrix, respectively,

$$\begin{aligned} A_\mu^i &= \bar{q} \gamma_\mu \gamma_5 \frac{\lambda^i}{2} q, \quad V_\mu^{em} = \bar{q} \gamma_\mu Q q, \\ Q &= \frac{1}{3} \text{diag}(2, -1, -1), \end{aligned} \quad (1.1)$$

where q collects the u, d and s quark fields,

$$q = \begin{pmatrix} u \\ d \\ s \end{pmatrix}. \quad (1.2)$$

It is very convenient to collect all Green functions in the generating functional whose properties may then be studied in a general manner. The construction goes as follows. One equips the QCD Lagrangian with external c -number fields v_μ, a_μ, s and p ,

$$\mathcal{L} = \mathcal{L}_{QCD}^0 + \bar{q} \gamma^\mu (v_\mu + \gamma_5 a_\mu) q - \bar{q} (s - i \gamma_5 p) q. \quad (1.3)$$

\mathcal{L}_{QCD}^0 is the Lagrangian with the masses of the three light quarks set to zero. The external fields v_μ, a_μ, s and p are hermitian 3×3 matrices in flavour space, and the quark mass matrix

$$\mathcal{M} = \text{diag}(m_u, m_d, m_s) \quad (1.4)$$

is contained in the scalar field s . The generating functional is the logarithm of the vacuum transition amplitude,

$$e^{iZ[v, a, s, p]} = \langle 0 \text{ out} | 0 \text{ in} \rangle, \quad (1.5)$$

and contains the external fields as arguments. Expanding Z in powers of v_μ, a_μ, s and p generates the connected Green functions of the quark currents. For example, the matrix element for $\pi\pi$ scattering is contained in the quartic term

$$\begin{aligned} Z &= \dots + \frac{i^3}{4!} \int dx_1 dx_2 dx_3 dx_4 a_\mu^i(x_1) a_\nu^k(x_2) a_\rho^l(x_3) a_\sigma^m(x_4) \times \\ &\quad \times \langle 0 | T A_i^\mu(x_1) A_k^\nu(x_2) A_l^\rho(x_3) A_m^\sigma(x_4) | 0 \rangle + \dots, \end{aligned} \quad (1.6)$$

with $a_\mu = a_\mu^b \frac{\lambda^b}{2}$.

Notice that the Lagrangian (1.3) is symmetric under local $SU(3)_L \times SU(3)_R$ transformations,

$$\begin{aligned} q &\rightarrow g_R \frac{1}{2}(1 + \gamma_5)q + g_L \frac{1}{2}(1 - \gamma_5)q , \\ g_{R,L} &\in SU(3)_{R,L} , \end{aligned} \quad (1.7)$$

provided the external fields are transformed accordingly,

$$\begin{aligned} r_\mu = v_\mu + a_\mu &\rightarrow g_R r_\mu g_R^\dagger + i g_R \partial_\mu g_R^\dagger , \\ l_\mu = v_\mu - a_\mu &\rightarrow g_L l_\mu g_L^\dagger + i g_L \partial_\mu g_L^\dagger , \\ s + ip &\rightarrow g_R (s + ip) g_L^\dagger . \end{aligned} \quad (1.8)$$

Here we consider only the case where the fields a_μ, v_μ are traceless,

$$\langle v_\mu \rangle = \langle a_\mu \rangle = 0 , \quad (1.9)$$

where $\langle A \rangle$ denotes the trace of the matrix A .

In the following we show how, in the framework of CHPT, the generating functional can be evaluated at low energies in a systematic manner.

2 Effective low-energy theory

The generating functional admits an expansion in powers of external momenta and of quark masses [1, 2, 3]. This expansion is most conveniently carried out in an effective theory, where the quark and gluon fields of QCD are replaced by a set of pseudoscalar fields which describe the degrees of freedom of the Goldstone bosons π, K and η . On the level of this effective theory, the expansion amounts to a derivative expansion of the effective Lagrangian. Counting the quark mass as two powers of the momenta, the expansion starts at order $O(p^2)$ and is of the form

$$\mathcal{L}_{eff} = \mathcal{L}_2 + \mathcal{L}_4 + \dots \quad (2.1)$$

The effective Lagrangian generates the corresponding expansion of the generating functional,

$$Z = Z_2 + Z_4 + \dots \quad (2.2)$$

This procedure to analyse the low-energy structure of the Green functions is called “chiral perturbation theory”. If the effective Lagrangian is chosen properly, the resulting Green functions are identical to the ones in the Standard Model [1, 3].

To see how this works in detail, it is convenient to collect the pseudoscalar fields in a unitary 3×3 matrix,

$$U = \exp(i\sqrt{2}\Phi/F) , \quad \Phi = \begin{pmatrix} \frac{\pi^0}{\sqrt{2}} + \frac{\eta_8}{\sqrt{6}} & \pi^+ & K^+ \\ \pi^- & -\frac{\pi^0}{\sqrt{2}} + \frac{\eta_8}{\sqrt{6}} & K^0 \\ K^- & \bar{K}^0 & -\frac{2\eta_8}{\sqrt{6}} \end{pmatrix} . \quad (2.3)$$

The *leading-order term* in the low-energy expansion is then generated by the tree diagrams of the non-linear σ model coupled to the external fields v, a, s and p ,

$$\mathcal{L}_2 = \frac{F^2}{4} \langle D_\mu U D^\mu U^\dagger + \chi U^\dagger + \chi^\dagger U \rangle , \quad (2.4)$$

where

$$D_\mu U = \partial_\mu U - i r_\mu U + i U l_\mu , \quad \chi = 2B(s + ip) . \quad (2.5)$$

The effective Lagrangian contains only two parameters at this order in the energy expansion: the pion decay constant in the chiral limit, $F \simeq 93$ MeV, and B , which is related to the quark condensate, $\langle 0 | \bar{u}u | 0 \rangle = -F^2 B [1 + O(m_{quark})]$. The constant B always appears multiplied by quark masses. At $O(p^2)$, the product $B m_{quark}$ can be expressed in terms of meson masses, e.g.,

$$\begin{aligned} M_{\pi^+}^2 &= B(m_u + m_d) + O(m_{quark}^2) , \\ M_{K^+}^2 &= B(m_u + m_s) + O(m_{quark}^2) . \end{aligned} \quad (2.6)$$

The fields U, v, a, s and p that occur in the effective Lagrangian are subject to the following chiral counting rules ²,

$$\begin{aligned} U &\sim O(p^0) , \\ D_\mu U, v_\mu, a_\mu &\sim O(p) , \\ s, p &\sim O(p^2) . \end{aligned} \quad (2.7)$$

Therefore, the *leading-order* effective Lagrangian \mathcal{L}_2 is of order p^2 . Furthermore, we note that \mathcal{L}_2 is invariant under the local transformation (1.8), provided the field U is transformed as

$$U \rightarrow g_R U g_L^\dagger . \quad (2.8)$$

The tree graphs generated by the Lagrangian (2.4) reproduce the soft pion theorems for mesons [5] in a concise manner. To illustrate, we consider the matrix element for elastic scattering of two charged pions,

$$\begin{aligned} &\langle \pi^+(p'_2) \pi^-(p'_1) \text{ out} | \pi^+(p_2) \pi^-(p_1) \text{ in} \rangle = \\ &4(2\pi)^6 p_2^0 p_1^0 \delta^3(\mathbf{p}'_2 - \mathbf{p}_2) \delta^3(\mathbf{p}'_1 - \mathbf{p}_1) + i(2\pi)^4 \delta^4(p'_1 + p'_2 - p_1 - p_2) T(s, t) , \end{aligned} \quad (2.9)$$

where $s = (p_1 + p_2)^2, t = (p'_1 - p_1)^2$ are the standard Mandelstam variables. There is only one diagram to evaluate, see Fig. 1. The result is

$$T(s, t) = \frac{s + t - 2M_\pi^2}{F^2} + O(p^4) . \quad (2.10)$$

Here the symbol $O(p^4)$ collects terms of order $O(p^4, p^2 m_{quark}, m_{quark}^2)$. The result (2.10) is due to Weinberg [6] who used current algebra and PCAC to analyse the Ward identities for the four-point function of the axial current. The effective Lagrangian calculation is very simple – the result is the same.

At *next-to-leading order*, the generating functional consists of three terms [2] :

²For a different counting see Ref. [4].

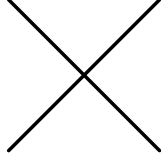


Figure 1: The Feynman diagram that generates the leading-order contribution (2.10) to the $\pi\pi$ scattering amplitude.

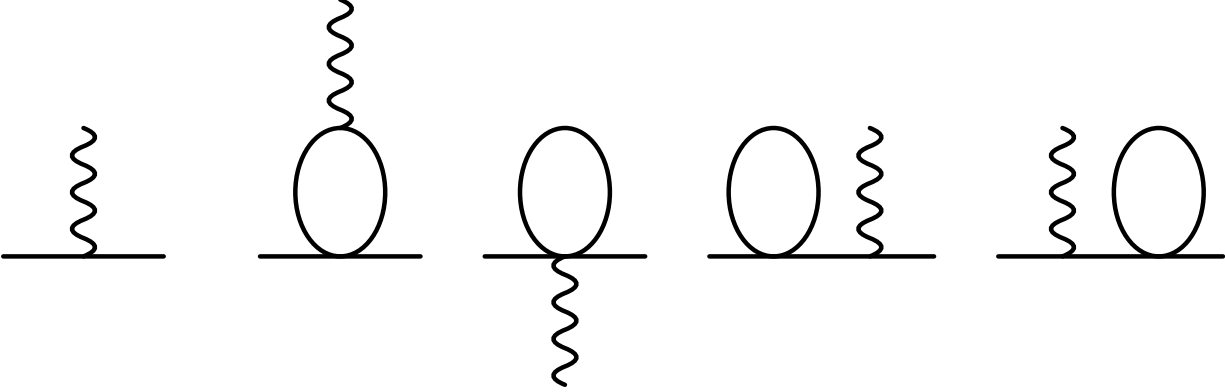


Figure 2: The tree and one-loop graphs, generated by \mathcal{L}_2 , that contribute to the electromagnetic form factor of the charged pion. π , K and η are running in the loops. The wiggly line denotes the electromagnetic current.

- i) The one-loop graphs generated by the lowest-order Lagrangian \mathcal{L}_2 .
- ii) An explicit local action of order p^4 .
- iii) A contribution to account for the chiral anomaly.

We briefly discuss these three contributions in turn and start with the one-loop graphs.

2.1 One-loop graphs

For illustration, we consider the electromagnetic form factor F_V^π of the pion,

$$\langle \pi^+(p') | V_\mu^{em}(0) | \pi^+(p) \rangle = (p' + p)_\mu F_V^\pi(t) \ ; \ t = (p' - p)^2 \ . \quad (2.11)$$

We display in Fig. 2 the relevant tree and one-loop graphs generated by \mathcal{L}_2 .

The leading-order term (tree graph of \mathcal{L}_2) is trivial, because $eF_V^\pi(0)$ is the charge of the pion,

$$F_V^{\pi,tree} = 1 \ . \quad (2.12)$$

The one-loop graphs are ultraviolet divergent, and a regularization scheme is needed. Although the final result is independent of the regularization chosen, it is very convenient to use dimensional regularization for the following reason. In this scheme, the chiral symmetry

of the effective theory is maintained, and only chiral symmetric counterterms are needed to cancel the divergences. Furthermore, because no new scale is introduced, the one-loop graphs are suppressed by two powers of the momenta relative to the tree diagrams [1], see also subsection 2.5. The result for the electromagnetic form factor is

$$\begin{aligned} F_V^{\pi, one\ loop}(t) &= 2\phi(t, M_\pi; d) + \phi(t, M_K; d) \ , \\ \phi(t, M; d) &= -\frac{tM^{d-4}}{(4\pi)^{d/2}} \frac{\Gamma(2 - \frac{d}{2})}{2F^2} \int_0^1 dx \, x(1-2x) \left[1 - \frac{t}{M^2}x(1-x) \right]^{\frac{d-4}{2}} \ , \end{aligned} \quad (2.13)$$

where we have indicated the dependence of the loop functions ϕ on the dimension d of space-time. From this representation of ϕ it is explicitly seen that the loop contribution is of order p^2 and is therefore suppressed by two powers of the momenta with respect to the tree level result $F_V^{\pi, tree} = 1$. Notice that ϕ is independent of any renormalization scale μ by construction – the loop integrals only involve internal as well as external momenta and the masses of the pions and kaons. As long as d is not an integer, the result is finite. When $d \rightarrow 4$, the loop functions develop a pole,

$$\phi(t, M; d) \xrightarrow{d \rightarrow 4} -\frac{t}{96\pi^2 F^2 (d-4)} + O(1) \ . \quad (2.14)$$

An analogous result holds for all Green functions evaluated at next-to-leading order: as long as d is different from 4, the result is finite—ultraviolet singularities only show up when $d \rightarrow 4$. These singularities are cancelled by the contributions from the local action at order p^4 to which we now turn.

2.2 Local action at order p^4

To the loop diagrams discussed above, one has to add the tree diagrams from $\mathcal{L}_2 + \mathcal{L}_4$ with one vertex from \mathcal{L}_4 and any number of vertices from \mathcal{L}_2 . The explicit form of \mathcal{L}_4 is [2]

$$\begin{aligned} \mathcal{L}_4 &= L_1 \langle D_\mu U^\dagger D^\mu U \rangle^2 + L_2 \langle D_\mu U^\dagger D_\nu U \rangle \langle D^\mu U^\dagger D^\nu U \rangle \\ &+ L_3 \langle D_\mu U^\dagger D^\mu U D_\nu U^\dagger D^\nu U \rangle + L_4 \langle D_\mu U^\dagger D^\mu U \rangle \langle \chi^\dagger U + \chi U^\dagger \rangle \\ &+ L_5 \langle D_\mu U^\dagger D^\mu U (\chi^\dagger U + U^\dagger \chi) \rangle + L_6 \langle \chi^\dagger U + \chi U^\dagger \rangle^2 + L_7 \langle \chi^\dagger U - \chi U^\dagger \rangle^2 \\ &+ L_8 \langle \chi^\dagger U \chi^\dagger U + \chi U^\dagger \chi U^\dagger \rangle - iL_9 \langle F_R^{\mu\nu} D_\mu U D_\nu U^\dagger + F_L^{\mu\nu} D_\mu U^\dagger D_\nu U \rangle \\ &+ L_{10} \langle U^\dagger F_R^{\mu\nu} U F_{L\mu\nu} \rangle + L_{11} \langle F_{R\mu\nu} F_R^{\mu\nu} + F_{L\mu\nu} F_L^{\mu\nu} \rangle + L_{12} \langle \chi^\dagger \chi \rangle \ , \end{aligned} \quad (2.15)$$

where

$$\begin{aligned} F_R^{\mu\nu} &= \partial^\mu r^\nu - \partial^\nu r^\mu - i[r^\mu, r^\nu] \ , \\ F_L^{\mu\nu} &= \partial^\mu l^\nu - \partial^\nu l^\mu - i[l^\mu, l^\nu] \ . \end{aligned} \quad (2.16)$$

This is the most general Lagrangian of order p^4 that exhibits local gauge invariance in the form of Eqs. (1.8), (2.8) , Lorentz invariance, P and C . The equation of motion has

furthermore been used to reduce the number of terms. The twelve new low-energy couplings L_1, \dots, L_{12} are divergent (except L_3 and L_7). They absorb the divergences of the one-loop graphs. Consider for illustration again the electromagnetic form factor F_V^π . It receives a contribution from L_9 ,

$$F_V^{\pi, \mathcal{L}^4}(t) = \frac{2L_9 t}{F^2} . \quad (2.17)$$

The sum $F_V^{\pi, one\ loop} + F_V^{\pi, \mathcal{L}^4}$ of the one-loop graphs and the counterterm contribution is finite, provided L_9 is appropriately tuned when $d \rightarrow 4$,

$$\begin{aligned} L_9 &= L_9^r(\mu) + \frac{\lambda(\mu)}{4} , \\ \lambda(\mu) &= (4\pi)^{-2} \mu^{d-4} \left\{ \frac{1}{d-4} - \frac{1}{2} (\ln(4\pi) + \Gamma'(1) + 1) \right\} , \end{aligned} \quad (2.18)$$

where the renormalized coupling $L_9^r(\mu)$ is finite when $d \rightarrow 4$. Here we have introduced a renormalization scale μ . Although the coupling constant L_9 does not know about this scale,

$$\mu \frac{dL_9}{d\mu} = 0 , \quad (2.19)$$

the individual pieces in the splitting (2.18) do depend on it,

$$\mu \frac{d\lambda}{d\mu} = \frac{1}{16\pi^2} + O(d-4) , \quad \mu \frac{dL_9^r}{d\mu} = -\frac{\mu}{4} \frac{d\lambda}{d\mu} . \quad (2.20)$$

Renormalization is now performed by writing

$$\phi(t, M; d) = \phi^{ren}(t, M, \mu; d) - \frac{t\lambda(\mu)}{6F^2} , \quad (2.21)$$

such that the complete expression for the formfactor becomes

$$F_V^\pi(t) = 1 + 2\phi^{ren}(t, M_\pi, \mu; d) + \phi^{ren}(t, M_K, \mu; d) + \frac{2L_9^r t}{F^2} + O(p^4) . \quad (2.22)$$

F_V^π approaches a finite limit when $d \rightarrow 4$ and is scale independent by construction. For illustration, we display the renormalized loop integral ³ at $d = 4$,

$$\begin{aligned} \phi^{ren}(t, M, \mu; 4) &= \frac{t}{32\pi^2 F^2} \int_0^1 dx \, x(1-2x) \log \left[1 - \frac{t}{M^2} x(1-x) \right] \\ &- \frac{t}{192\pi^2 F^2} \left\{ \log \frac{M^2}{\mu^2} + 1 \right\} . \end{aligned} \quad (2.23)$$

Note that, as is required by unitarity, the function ϕ contains a branch point at $t = 4M^2$. The expression (2.23) is not expanded further in powers of t/M^2 , because this would result in a Taylor series that is valid only in the range $|t| < 4M^2$. Stated differently, the momentum and quark expansion is performed at a fixed value of the ratio p^2/m_{quark} .

³The combination $\phi^{ren}(t, M_\pi, \mu; 4) + \frac{2L_9^r t}{3F^2}$ is denoted by $H_{\pi\pi}$ in Refs. [7, 8].

Table 1: Phenomenological values and source for the renormalized coupling constants $L_i^r(M_\rho)$. The quantities Γ_i in the fourth column determine the scale dependence of the $L_i^r(\mu)$ according to Eq. (2.25). L_{11}^r and L_{12}^r are not directly accessible to experiment.

i	$L_i^r(M_\rho) \times 10^3$	source	Γ_i
1	0.4 ± 0.3	$K_{e4}, \pi\pi \rightarrow \pi\pi$	3/32
2	1.35 ± 0.3	$K_{e4}, \pi\pi \rightarrow \pi\pi$	3/16
3	-3.5 ± 1.1	$K_{e4}, \pi\pi \rightarrow \pi\pi$	0
4	-0.3 ± 0.5	Zweig rule	1/8
5	1.4 ± 0.5	$F_K : F_\pi$	3/8
6	-0.2 ± 0.3	Zweig rule	11/144
7	-0.4 ± 0.2	Gell-Mann–Okubo, L_5, L_8	0
8	0.9 ± 0.3	$M_{K^0} - M_{K^+}, L_5,$ $(2m_s - m_u - m_d) : (m_d - m_u)$	5/48
9	6.9 ± 0.7	$\langle r^2 \rangle_V^\pi$	1/4
10	-5.5 ± 0.7	$\pi \rightarrow e\nu\gamma$	-1/4
11			-1/8
12			5/24

The same procedure carries over to all Green functions collected in the generating functional: they remain finite when $d \rightarrow 4$, provided the low-energy couplings L_i are appropriately tuned in this limit,

$$L_i = L_i^r(\mu) + \Gamma_i \lambda(\mu) . \quad (2.24)$$

The coefficients Γ_i have been evaluated in [2] and are displayed in table 1. The couplings L_i are independent of the renormalization scale μ – therefore, the Green functions do not depend on it either. The scale dependence of the renormalized, finite couplings $L_i^r(\mu)$ is governed by the coefficients Γ_i ,

$$L_i^r(\mu_2) = L_i^r(\mu_1) + \frac{\Gamma_i}{16\pi^2} \ln \frac{\mu_1}{\mu_2} . \quad (2.25)$$

The constants F, B , together with L_1^r, \dots, L_{10}^r , completely determine the low-energy behaviour of pseudoscalar meson interactions to $O(p^4)$. L_{11}^r and L_{12}^r are contact terms that are not directly accessible to experiment. We discuss the value of the low-energy constants L_1^r, \dots, L_{10}^r below.

2.3 Chiral anomaly

The effective Lagrangian $\mathcal{L}_2 + \mathcal{L}_4$ is invariant under the local $SU(3)_L \times SU(3)_R$ transformations (1.8), (2.8). Because dimensional regularization preserves this symmetry, the corresponding generating functional is invariant as well. On the other hand, the vacuum transition

amplitude is not invariant under the transformations (1.8) – it is afflicted with anomalies. (In technical terms, the relevant fermionic determinant does not allow for a chiral invariant regularization [9].) Consider infinitesimal transformations

$$g_R = 1 + i\alpha(x) + i\beta(x) \ , \ g_L = 1 + i\alpha(x) - i\beta(x) \ . \quad (2.26)$$

The conventions in the definition of the fermionic determinant may be chosen such that the generating functional is invariant under the transformations generated by the vector currents. The change in Z then only involves the difference $\beta(x)$ between g_R and g_L [10, 11],

$$\begin{aligned} \delta Z &= - \int dx \langle \beta(x) \Omega(x) \rangle \ , \\ \Omega(x) &= \frac{N_c}{16\pi^2} \epsilon^{\alpha\beta\mu\nu} \left[v_{\alpha\beta} v_{\mu\nu} + \frac{4}{3} D_\alpha a_\beta D_\mu a_\nu + \frac{2i}{3} \{v_{\alpha\beta}, a_{\mu a_\nu}\} \right. \\ &\quad \left. + \frac{8i}{3} a_\mu v_{\alpha\beta} a_\nu + \frac{4}{3} a_\alpha a_\beta a_\mu a_\nu \right] \ , \\ v_{\alpha\beta} &= \partial_\alpha v_\beta - \partial_\beta v_\alpha - i[v_\alpha, v_\beta] \ , \\ D_\alpha a_\beta &= \partial_\alpha a_\beta - i[v_\alpha, a_\beta] \ . \end{aligned} \quad (2.27)$$

(N_c is the number of colours and $\varepsilon_{0123} = 1$.) Notice that Ω only depends on the external fields v_μ and a_μ . The quark masses do not occur – the anomalies are independent thereof. A functional $Z[U, l, r]$ that reproduces the chiral anomaly was first constructed by Wess and Zumino [11]. For practical purposes, it is useful to write it in the explicit form given by Witten [12]:

$$Z[U, l, r]_{ZW} = -\frac{iN_c}{240\pi^2} \int_{M^5} d^5x \epsilon^{ijklm} \langle \Sigma_i^L \Sigma_j^L \Sigma_k^L \Sigma_l^L \Sigma_m^L \rangle \quad (2.28)$$

$$\begin{aligned} & -\frac{iN_c}{48\pi^2} \int d^4x \varepsilon_{\mu\nu\alpha\beta} \left(W(U, l, r)^{\mu\nu\alpha\beta} - W(\mathbf{1}, l, r)^{\mu\nu\alpha\beta} \right) \\ W(U, l, r)_{\mu\nu\alpha\beta} &= \langle U l_\mu l_\nu l_\alpha U^\dagger r_\beta + \frac{1}{4} U l_\mu U^\dagger r_\nu U l_\alpha U^\dagger r_\beta + i U \partial_\mu l_\nu l_\alpha U^\dagger r_\beta \\ & \quad + i \partial_\mu r_\nu U l_\alpha U^\dagger r_\beta - i \Sigma_\mu^L l_\nu U^\dagger r_\alpha U l_\beta + \Sigma_\mu^L U^\dagger \partial_\nu r_\alpha U l_\beta \\ & \quad - \Sigma_\mu^L \Sigma_\nu^L U^\dagger r_\alpha U l_\beta + \Sigma_\mu^L l_\nu \partial_\alpha l_\beta + \Sigma_\mu^L \partial_\nu l_\alpha l_\beta \\ & \quad - i \Sigma_\mu^L l_\nu l_\alpha l_\beta + \frac{1}{2} \Sigma_\mu^L l_\nu \Sigma_\alpha^L l_\beta - i \Sigma_\mu^L \Sigma_\nu^L \Sigma_\alpha^L l_\beta \rangle \\ & \quad - (L \leftrightarrow R) \ , \end{aligned} \quad (2.29)$$

$$\Sigma_\mu^L = U^\dagger \partial_\mu U \ , \ \Sigma_\mu^R = U \partial_\mu U^\dagger$$

$$N_c = 3 \ ,$$

where $(L \leftrightarrow R)$ stands for the interchange

$$U \leftrightarrow U^\dagger \ , \quad l_\mu \leftrightarrow r_\mu \ , \quad \Sigma_\mu^L \leftrightarrow \Sigma_\mu^R \ .$$

The first term in Eq. (2.28) bears the mark of the anomaly: this part of the action is local in *five* dimensions, but it cannot be written as a finite polynomial in U and $\partial_\mu U$ in four dimensions. This term involves at least five pseudoscalar fields and will not be needed in the

following chapters. It does contribute to K_{e5} decays, but its contribution is proportional to the electron mass and therefore strongly suppressed, see the section on K_{e5} decays [7]. The convention used in Eq. (2.28) ensures that $Z[U, l, r]_{WZW}$ conserves parity and reproduces the transformation law (2.27).

The Wess–Zumino–Witten functional contains all the anomalous contributions to electromagnetic and semileptonic weak meson decays. The relevant piece for, e.g., K_{l4} decays is

$$Z[U, l, r]_{WZW} = \frac{i\sqrt{2}}{4\pi^2 F^3} \int d^4x \epsilon_{\mu\nu\rho\sigma} \langle \partial^\mu \Phi \partial^\nu \Phi \partial^\rho \Phi v^\sigma \rangle + \dots \quad (2.30)$$

Furthermore, all Ward identities originating from the $SU(3)_L \times SU(3)_R$ transformation properties of the underlying theory may be derived from the fact that i) the difference $Z - Z_{WZW}$ is invariant under local gauge transformations, and ii) Z_{WZW} transforms in the manner indicated in Eq. (2.27).

2.4 The low–energy constants L_i

Similarly to F and B in the lowest–order Lagrangian \mathcal{L}_2 , the low–energy constants L_i^r are not constrained by chiral symmetry – they are fixed by the dynamics of the underlying theory in terms of the renormalization group invariant scale Λ and the heavy quark masses m_c, m_b, \dots . With present techniques, it is however not possible to evaluate them directly from the QCD Lagrangian (for some attempts in this direction see Ref. [13]). Therefore, they have been determined by comparison with experimental low–energy information and by using large– N_c arguments. The result is shown in column 2 of table 1, where L_1^r, \dots, L_{10}^r are displayed at the scale $\mu = M_\rho$. The experimental information underlying these values is shown in column 3. L_1, L_2 and L_3 are taken from a recent overall fit to K_{e4} and $\pi\pi$ data [14], see also Refs. [15, 16] and the section on K_{l4} decays in [7]. L_4, \dots, L_{10} are from [2]. For L_9 see also [17]. The combination $L_9 + L_{10}$ has also been determined in [18] from data on $\gamma\gamma \rightarrow \pi^+\pi^-$.

Once the low–energy couplings L_i^r are known, the machinery set up above allows one to make predictions. As a simple example consider the charge radius of the electromagnetic form factor,

$$F_V^\pi(t) = 1 + \frac{1}{6} \langle r^2 \rangle_V^\pi t + O(t^2) \quad (2.31)$$

The expression for $\langle r^2 \rangle_V^\pi$ follows easily from Eqs. (2.22) and (2.23),

$$\langle r^2 \rangle_V^\pi = \frac{12L_9^r}{F^2} - \frac{1}{32\pi^2 F^2} \left\{ 2 \log \frac{M_\pi^2}{\mu^2} + \log \frac{M_K^2}{\mu^2} + 3 \right\} + O(m_{quark}) \quad (2.32)$$

Here, the symbol $O(m_{quark})$ stands for higher–order contributions which are not worked out here (two loops and beyond). Therefore, the constant L_9^r may be pinned down from the experimental value [19] $\langle r^2 \rangle_V^\pi = 0.439 \pm 0.008 \text{ fm}^2$. The same constant occurs [7, 8] in the slope λ_+ of the form factor $f_+^{K\pi}(t)$ measured in K_{e3}^0 decay [20],

$$\lambda_+ = 0.0286 \pm 0.0022 \quad (2.33)$$

Table 2: Occurrence of the low-energy coupling constants L_1, \dots, L_{10} and of the anomaly in the semileptonic decays discussed in [7]. In $K_{\mu 4}$ decays, the same constants as in the electron mode (displayed here) occur. In addition, L_6 and L_8 enter in the channels $K^+ \rightarrow \pi^+ \pi^- \mu^+ \nu_\mu$ and $K^+ \rightarrow \pi^0 \pi^0 \mu^+ \nu_\mu$.

	$K_{l2\gamma}$	K_{l2ll}	K_{l3}	$K_{l3\gamma}$	$K^+ \rightarrow \pi^+ \pi^- e^+ \nu_e$	$K^+ \rightarrow \pi^0 \pi^0 e^+ \nu_e$	$K^0 \rightarrow \pi^0 \pi^- e^+ \nu_e$
L_1					\times	\times	
L_2					\times	\times	
L_3					\times	\times	\times
L_4					\times	\times	
L_5					\times	\times	\times
L_9		\times	\times	\times	\times	\times	\times
$L_9 + L_{10}$	\times	\times		\times			
Anomaly	\times	\times		\times	\times		\times

Inserting $L_9^r = 6.9 \cdot 10^{-3}$ in the expression for λ_+ gives for the central value the prediction

$$\lambda_+ = 0.031 \quad . \quad (2.34)$$

We see that the machine works properly. For a more thorough discussion of charge radii in the meson sector we refer the reader to Refs. [7, 8]. Many more predictions have been worked out – for reviews see, e.g., Ref. [21]. The semileptonic decays which will be measured with high precision at DAΦNE provide the opportunity to expose the method to very thorough consistency checks. We display for this purpose in table 2 the low-energy couplings that occur in the matrix elements of the semileptonic kaon decays discussed in [7]. (There is an ambiguity concerning the bookkeeping of L_4 and L_5 : some of these contributions may be absorbed into the physical decay constants F_π, F_K . Here we have chosen the convention that corresponds to the amplitudes displayed in [7]. Furthermore, in K_{e5} decays, additional constants may occur. The relevant one-loop corrections have however not been worked out yet. This channel is therefore omitted in the table.)

Are these values of the low-energy constants consistent with the general picture underlying the chiral perturbative analysis or are they unduly large? Consider the charge radius of the electromagnetic form factor worked out above. If the pion and kaon cuts were the only low-energy singularities of importance, we would expect the main contribution to the charge radius to stem from the chiral logarithms and the contribution from L_9 to be negligible. With a scale μ somewhere in the range from 500 MeV to 1 GeV gives $\langle r^2 \rangle_V^\pi = 0.03 \dots 0.09 \text{ fm}^2$ from the curly bracket in Eq. (2.32), clearly outside the experimental value. Therefore, the coupling L_9 generates the main contribution. On the other hand, the observed value of the radius is consistent with ρ dominance, $\langle r^2 \rangle_V^\pi \simeq 6M_\rho^{-2} = 0.4 \text{ fm}^2$. To understand the size of L_9 one therefore needs to understand how the presence of an excited $q\bar{q}$ state at $M_\rho = 770$ MeV affects the low-energy structure of the Green functions [2]. This will be discussed in some detail in subsection 3.

2.5 Chiral power counting

Power counting in the low-energy expansion may be discussed in a concise manner as follows [1]. Take a fixed term in the expansion of the generating functional in powers of the external fields – an example is given in Eq. (1.6). Let us further consider a fixed, connected L -loop diagram that contributes to this term. Since all internal lines correspond to pseudoscalar mesons, the finite part of the loop integral is a homogeneous function of the external momenta, the meson masses and the renormalization scale μ . Denote by D_L the degree of homogeneity, and by D_F the number of external fields times their dimension according to (2.7) (i.e., $D_F = 4$ in the present case). We call

$$D = D_L + D_F \quad (2.35)$$

the *chiral dimension* of the L -loop amplitude.

For a general connected L -loop diagram with N_d vertices of $O(p^d)$ ($d = 2, 4, \dots$), it is given by [1]

$$D = 2L + 2 + \sum_d (d-2)N_d, \quad d = 2, 4, \dots \quad (2.36)$$

and therefore, up to $O(p^4)$:

$$\begin{aligned} D = 2: \quad L = 0, d = 2 & \quad Z_2 = \int d^4x \mathcal{L}_2 \\ D = 4: \quad L = 0, d = 4 & \quad Z_4^{\text{tree}} = \int d^4x \mathcal{L}_4 + Z_{WZW} \\ L = 1, d = 2 & \quad Z_4^{L=1} \text{ for } \mathcal{L}_2. \end{aligned} \quad (2.37)$$

To verify, we consider the case of the $\pi\pi$ scattering amplitude at tree level: in addition to the amplitude (2.10) of homogeneity 2, the Green function (1.6) contains four external propagators and four (derivative) couplings to the axial currents. Therefore, $D_L = 2 + 4 * (-2 + 1) = -2$, $D_F = 4$, such that $D = 2$.

This is true for each term in the expansion (1.6), such that

$$Z = Z_2 + Z_4^{\text{tree}} + Z_4^{L=1} + O(p^6). \quad (2.38)$$

For a given Green function, the chiral dimension D increases with L according to Eq. (2.36). In order to reproduce the (fixed) physical dimension of the amplitude, each loop produces a factor $1/F^2$. Together with the geometric loop factor $(4\pi)^{-2}$, the loop expansion suggests

$$4\pi F_\pi = 1.2 \text{ GeV} \quad (2.39)$$

as the natural scale of the chiral expansion [22]. Restricting the domain of applicability of CHPT to momenta $|p| \lesssim O(M_K)$, the natural expansion parameter of chiral amplitudes is expected to be of the order

$$\frac{M_K^2}{16\pi^2 F_\pi^2} = 0.18. \quad (2.40)$$

In addition, these terms often occur multiplied with chiral logarithms. It is, therefore, no surprise that substantial higher-order corrections in the chiral expansion are the rule rather than the exception in the framework of $SU(3) \times SU(3)$. On the other hand, for $SU(2) \times SU(2)$ and for momenta $|p| \lesssim O(M_\pi)$ the chiral expansion is expected to converge considerably faster.

3 Meson resonances in CHPT

We now discuss the singularities generated by the exchange of nearby resonances like the rho, omega, phi etc. and their effect on the low-energy structure of the Green functions. A systematic analysis of the couplings between meson resonances of the type V , A , S , P and the pseudoscalar mesons was performed in Ref. [23] (see also Ref. [24] for related work).

It is straightforward to couple general matter fields to the Goldstone modes using the methods of non-linear realizations of the chiral group $G = SU(3)_L \times SU(3)_R$ [25]. The chiral transformation properties of the resonance fields depend only on their transformation properties under the diagonal subgroup $SU(3)_V$. A non-linear realization of spontaneously broken chiral symmetry is defined [25] by specifying the action of G on the elements $u(\phi)$ of the coset space $SU(3)_L \times SU(3)_R / SU(3)_V$:

$$u(\phi) \xrightarrow{G} g_R u(\phi) h(g, \phi)^\dagger = h(g, \phi) u(\phi) g_L^\dagger, \quad (3.1)$$

where ϕ^i ($1 \leq i \leq 8$) are the Goldstone fields of Eq. (2.3). In the usual convention, the relation between $u(\phi)$ and $U(\phi)$ in Eq. (2.3) is simply

$$U(\phi) = u(\phi)^2. \quad (3.2)$$

The so-called compensating $SU(3)_V$ transformation $h(g, \phi)$ defined by Eq. (3.1) allows the construction of an arbitrary non-linear realization of G . For instance, an octet

$$R = \frac{1}{\sqrt{2}} \lambda_a R^a \quad (3.3)$$

of resonance fields transforms as

$$R \xrightarrow{G} h(g, \phi) R h(g, \phi)^\dagger. \quad (3.4)$$

Here, we shall only discuss V and A resonances, referring to [23] for all details including the treatment of S and P resonances.

3.1 Antisymmetric tensor field formulation

We describe the V and A mesons by antisymmetric tensor fields $R_{\mu\nu} = -R_{\nu\mu}$ [2, 23]. Alternative treatments of spin-1 fields are considered below. The tensor field formulation is especially convenient for including the interactions with external gauge fields. Another advantage is that even in the presence of interactions the spin-1 character of the field is not modified. This is in contrast to the vector field formulation where couplings of the form $V_\mu \partial^\mu S$ with a scalar field S may arise requiring a redefinition of the spin-1 vector field. A well-known example of this type is a_1 - π mixing.

It turns out [23] that for V and A resonances only octets can contribute to the L_i . For the kinetic terms we define a covariant derivative

$$\nabla_\mu R = \partial_\mu R + [\Gamma_\mu, R], \quad (3.5)$$

with a connection

$$\Gamma_\mu = \frac{1}{2} \{u^\dagger (\partial_\mu - i r_\mu) u + u (\partial_\mu - i l_\mu) u^\dagger\} \quad (3.6)$$

ensuring the proper transformation

$$\nabla_\mu R \xrightarrow{G} h(g, \phi) \nabla_\mu R h(g, \phi)^\dagger. \quad (3.7)$$

Invoking P and C invariance, one finds that all couplings linear in the fields V , A , S and P start at order p^2 . The complete resonance Lagrangian of lowest order [23]

$$\mathcal{L}_{\text{res}} = \sum_{R=V,A,S,P} \{\mathcal{L}_{\text{kin}}(R) + \mathcal{L}_2(R)\}, \quad (3.8)$$

consists of kinetic terms

$$\mathcal{L}_{\text{kin}}(R) = -\frac{1}{2} \langle \nabla^\lambda R_{\lambda\mu} \nabla_\nu R^{\nu\mu} - \frac{M_R^2}{2} R_{\mu\nu} R^{\mu\nu} \rangle \quad R = V, A, \quad (3.9)$$

where M_R are the corresponding masses in the chiral limit, and of interaction Lagrangians

$$\mathcal{L}_2[V(1^{--})] = \frac{F_V}{2\sqrt{2}} \langle V_{\mu\nu} f_+^{\mu\nu} \rangle + \frac{iG_V}{\sqrt{2}} \langle V_{\mu\nu} u^\mu u^\nu \rangle \quad (3.10)$$

$$\begin{aligned} \mathcal{L}_2[A(1^{++})] &= \frac{F_A}{2\sqrt{2}} \langle A_{\mu\nu} f_-^{\mu\nu} \rangle \\ f_\pm^{\mu\nu} &= u F_L^{\mu\nu} u^\dagger \pm u^\dagger F_R^{\mu\nu} u. \end{aligned} \quad (3.11)$$

The coupling constants F_V , G_V and F_A are real. As already mentioned, we only exhibit the V and A Lagrangians here.

The coupling constants F_V , G_V and F_A (and the corresponding ones for S , P resonances) can be estimated from resonance decays, see [23] for details. We use

$$\begin{aligned} |F_V| &= 154 \text{ MeV} & |G_V| &= 53 \text{ MeV} \\ |F_A| &= 123 \text{ MeV} & M_A &= 968 \text{ MeV} \end{aligned} \quad (3.12)$$

together with $M_V = M_\rho$.

Resonance exchange (more specifically, here V and A exchange only) then gives rise to the following contributions to the L_i [23] :

$$\begin{aligned} L_1^V &= \frac{G_V^2}{8M_V^2} & L_2^V &= 2L_1^V & L_3^V &= -6L_1^V \\ L_9^V &= \frac{F_V G_V}{2M_V^2} & L_{10}^V &= -\frac{F_V^2}{4M_V^2} & L_{10}^A &= \frac{F_A^2}{4M_A^2}. \end{aligned} \quad (3.13)$$

The resulting L_i are summarized in table 3, which compares the different resonance exchange contributions with the phenomenologically determined values of the $L_i^r(M_\rho)$. For vector and axial-vector mesons only the $SU(3)$ octets contribute, whereas both octets and singlets are relevant in the case of scalar and pseudoscalar resonances.

The results displayed in table 3 can be summarized in the following way:

Table 3: V , A , S , S_1 and η_1 contributions to the coupling constants L_i^r in units of 10^{-3} . The last column shows the results obtained with the relations (3.15) in the minimal model of V , A resonance couplings.

i	$L_i^r(M_\rho)$	V	A	S	S_1	η_1	Total	MM ^{c)}
1	0.4 ± 0.3	0.6	0	-0.2	$0.2^b)$	0	0.6	0.9
2	1.35 ± 0.3	1.2	0	0	0	0	1.2	1.8
3	-3.5 ± 1.1	-3.6	0	0.6	0	0	-3.0	-4.9
4	-0.3 ± 0.5	0	0	-0.5	$0.5^b)$	0	0.0	0.0
5	1.4 ± 0.5	0	0	$1.4^a)$	0	0	1.4	1.4
6	-0.2 ± 0.3	0	0	-0.3	$0.3^b)$	0	0.0	0.0
7	-0.4 ± 0.2	0	0	0	0	-0.3	-0.3	-0.3
8	0.9 ± 0.3	0	0	$0.9^a)$	0	0	0.9	0.9
9	6.9 ± 0.7	$6.9^a)$	0	0	0	0	6.9	7.3
10	-5.5 ± 0.7	-10.0	4.0	0	0	0	-6.0	-5.5

^{a)} Input.

^{b)} Large- N_c estimate.

^{c)} With (3.15)

Chiral duality:

The $L_i^r(M_\rho)$ are practically saturated by resonance exchange. There is very little room left for additional contributions.

Chiral VMD:

Whenever spin-1 resonances can contribute at all ($i = 1, 2, 3, 9, 10$), the $L_i^r(M_\rho)$ are almost completely dominated by V (and for L_{10} only, also A) exchange. In particular, the strong V , A exchange contributions are responsible for the relatively large coupling constants L_3 , L_9 and L_{10} .

3.2 Alternative descriptions for spin-1 fields

The use of antisymmetric tensor fields to describe spin-1 resonances is just a matter of convenience. In fact, the high-energy structure of QCD allows to establish a complete equivalence between different formulations and it gives rise to additional information [26] :

- Imposing the QCD constraints at high energies via dispersion relations, all phenomenologically successful models for V , A resonances are equivalent to $O(p^4)$: tensor field description used in Eqs. (3.9), (3.10), (3.11), massive Yang-Mills [27], hidden-gauge formulations [28], etc.
- With additional QCD-inspired assumptions of high-energy behaviour, like an unsubtracted dispersion relation for the pion form factor, all V and A couplings can be expressed in terms of F_π and M_ρ only:

$$\begin{aligned}
 F_V &= \sqrt{2}F_\pi & G_V &= F_\pi/\sqrt{2} \\
 F_A &= F_\pi & M_A &= \sqrt{2}M_V .
 \end{aligned} \tag{3.14}$$

The spin-1 resonance exchange contributions to the $O(p^4)$ chiral couplings are in this case

$$L_1^V = L_2^V/2 = -L_3^V/6 = L_9^V/8 = -L_{10}^{V+A}/6 = F_\pi^2/(16M_V^2) . \quad (3.15)$$

The last column in table 3 shows the predictions for the L_i using the relations (3.15). The agreement is quite remarkable.

The theoretical prediction $G_V = F_\pi/\sqrt{2}$ implies

$$\Gamma(\rho \rightarrow 2\pi) = \frac{M_\rho^3(1 - 4M_\pi^2/M_\rho^2)^{3/2}}{96\pi F_\pi^2} = 141 \text{ MeV} , \quad (3.16)$$

which is one version of the so-called KSFR relation [29]. This is a non-trivial result: higher-order terms in the chiral expansion could a priori influence the decay $\rho \rightarrow 2\pi$, but would be negligible at small momenta $|p| \lesssim M_K$. The underlying reason for the success of the KSFR relation is once again the intimate connection between the high-energy structure predicted by QCD and the low-energy structure of CHPT via dispersion relations [30].

The most compact way to exhibit the relations (3.14) in a Lagrangian form is by way of a “minimal model” [26] employing vector fields for the spin-1 resonances [27, 28] :

$$\begin{aligned} \mathcal{L}_{MM} &= -\frac{1}{4}\langle \bar{V}_{\mu\nu} \bar{V}^{\mu\nu} \rangle + \frac{1}{2}M_V^2 \left\langle \left(\bar{V}_\mu - \frac{2iF_\pi}{M_V} \Gamma_\mu \right)^2 \right\rangle \\ &\quad -\frac{1}{4}\langle \hat{A}_{\mu\nu} \hat{A}^{\mu\nu} \rangle + M_V^2 \left\langle \left(\hat{A}_\mu + \frac{F_\pi}{2M_V} u_\mu \right)^2 \right\rangle \\ \bar{V}_{\mu\nu} &= \partial_\mu \bar{V}_\nu - \partial_\nu \bar{V}_\mu - i\frac{M_V}{2F_\pi} [\bar{V}_\mu, \bar{V}_\nu] \\ \hat{A}_{\mu\nu} &= \nabla_\mu \hat{A}_\nu - \nabla_\nu \hat{A}_\mu . \end{aligned} \quad (3.17)$$

The vector field \bar{V}_μ transforms like a gauge field under chiral rotations,

$$\bar{V}_\mu \xrightarrow{G} h(g, \phi) \bar{V}_\mu h(g, \phi)^\dagger + \frac{2iF_\pi}{M_V} h(g, \phi) \partial_\mu h(g, \phi)^\dagger , \quad (3.18)$$

whereas the axial-vector field \hat{A}_μ transforms homogeneously as in Eq. (3.4).

This short introduction to CHPT (see Refs. [21, 31] for more extensive treatments with references to the original literature) contains all the ingredients necessary for the calculation of semileptonic K decay amplitudes to $O(p^4)$ [7]. The chiral realization of the non-leptonic weak interactions is discussed in [32].

Bibliography

- [1] S. Weinberg, Physica 96A (1979) 327.
- [2] J. Gasser and H. Leutwyler, Ann. Phys. 158 (1984) 142; Nucl. Phys. B250 (1985) 465.
- [3] H. Leutwyler, On the foundations of chiral perturbation theory, Univ. Bern preprint BUTP-93/24, to appear in Ann. of Phys.
- [4] N.H. Fuchs, H. Sazdjian and J. Stern, Phys. Lett. B269 (1991) 183;
J. Stern, H. Sazdjian and N.H. Fuchs, Phys. Rev. D47 (1993) 3814;
M. Knecht and J. Stern, Generalized chiral perturbation theory, this report.
- [5] For a review see, e.g., S.L. Adler and R.F. Dashen, Current Algebras and Applications to Particle Physics, W.A. Benjamin (New York, 1968).
- [6] S. Weinberg, Phys. Rev. Lett. 17 (1966) 616.
- [7] J. Bijnens et al., Semileptonic kaon decays, this report.
- [8] J. Gasser and H. Leutwyler, Nucl. Phys. B250 (1985) 517.
- [9] K. Fujikawa, Phys. Rev. D21 (1980) 2848;
A.P. Balachandran et al., Phys. Rev. D25 (1982) 2713.
- [10] W.A. Bardeen, Phys. Rev. 184 (1969) 1848.
- [11] J. Wess and B. Zumino, Phys. Lett. B37 (1971) 95.
- [12] E. Witten, Nucl. Phys. B223 (1983) 422; for further discussions see also
C.G. Callan and E. Witten, Nucl. Phys. B239 (1984) 161;
Ö. Kaymakçalan, S. Rajeev and J. Schechter, Phys. Rev. D30 (1984) 594;
K. Chou et al., Phys. Lett. B134 (1984) 67;
H. Kawai and S. Tye, Phys. Lett. B140 (1984) 403.
- [13] J. Bijnens, Introduction to extended Nambu–Jona-Lasinio models, this report;
R. Petronzio, Quark–resonance models, this report.
- [14] J. Bijnens, G. Colangelo and J. Gasser, K_{t4} decays beyond one loop, Bern University preprint BUTP-94/4, ROM2F 94/05 (hep-ph/9403390), to appear in Nucl. Phys. B.
- [15] J. Bijnens, Nucl. Phys. B337 (1990) 635.

- [16] C. Riggenbach, J. Gasser, J.F. Donoghue and B.R. Holstein, Phys. Rev. D43 (1991) 127.
- [17] J. Bijnens and F. Cornet, Nucl. Phys. B296 (1988) 557.
- [18] D. Babusci et al., Phys. Lett. B277 (1992) 158.
- [19] S.R. Amendolia et al., Nucl. Phys. B277 (1986) 168. The literature on the subject may be traced from this reference.
- [20] Review of Particle Properties, Phys. Rev. D50 (1994) vol. 3, part II.
- [21] J. Gasser, The QCD vacuum and chiral symmetry, in: Hadrons and Hadronic Matter, Eds. D. Vautherin et al., Plenum Publ. Co. (New York, 1990) ;
H. Leutwyler, Chiral effective Lagrangians, Lecture Notes in Physics, vol. 396, Eds. H. Mitter and H. Gausterer, Springer-Verlag (Berlin, 1991);
Nonperturbative methods, Proc. of the XXVI Int. Conference on High Energy Physics, Dallas, 1992, Ed. J.R. Sanford, American Inst. Phys. (New York, 1993);
Principles of Chiral Perturbation Theory, Lectures given at the Workshop “Hadron 94”, Gramado, RS, Brasil, BUTP-94/13 (hep-ph/9406283);
G. Ecker, Chiral perturbation theory, in: Quantitative Particle Physics: Cargèse 1992, Eds. M. Lévy et al., Plenum Publ. Co. (New York, 1993) ;
U.-G. Meißner, Recent developments in chiral perturbation theory, Rep. Prog. Phys. 56 (1993) 903;
A. Pich, Introduction to chiral perturbation theory, Lectures given at the 5th Mexican School of Particles and Fields, Guanajuato, Mexico, Dec. 1992, preprint CERN-TH.6978/93.
- [22] A.V. Manohar and H. Georgi, Nucl. Phys. B234 (1984) 189.
- [23] G. Ecker, J. Gasser, A. Pich and E. de Rafael, Nucl. Phys. B321 (1989) 311.
- [24] J.F. Donoghue, C. Ramirez and G. Valencia, Phys. Rev. D39 (1989) 1947;
M. Praszalowicz and G. Valencia, Nucl. Phys. B341 (1990) 27.
- [25] S. Coleman, J. Wess and B. Zumino, Phys. Rev. 177 (1969) 2239;
C. Callan, S. Coleman, J. Wess and B. Zumino, Phys. Rev. 177 (1969) 2247.
- [26] G. Ecker, J. Gasser, H. Leutwyler, A. Pich and E. de Rafael, Phys. Lett. B223 (1989) 425.
- [27] For a review see, e.g., U.-G. Meißner, Phys. Reports 161 (1988) 213.
- [28] M. Bando, T. Kugo and K. Yamawaki, Phys. Reports 164 (1988) 115.
- [29] K. Kawarabayashi and M. Suzuki, Phys. Rev. Lett. 16 (1966) 255;
Riazuddin and Fayyazuddin, Phys. Rev. 147 (1966) 1071.

- [30] G. Ecker, Vector mesons and chiral symmetry, in Proc. of the 12th Warsaw Symposium on Elementary Particle Physics, Kazimierz, Poland, June 1988, Eds. Z. Ajduk et al., World Scient. Publ. Co. (Singapore, 1990).
- [31] H. Georgi, Weak Interactions and Modern Particle Theory, Benjamin/Cummings (Menlo Park, 1984);
J.F. Donoghue, E. Golowich and B.R. Holstein, Dynamics of the Standard Model, Cambridge Univ. Press (Cambridge, 1992);
Proc. of the Workshop on Effective Field Theories of the Standard Model, Dobogókő, Hungary, Aug. 1991, Ed. U.-G. Meißner, World Scient. Publ. Co. (Singapore, 1992).
- [32] G. D'Ambrosio et al., Radiative non-leptonic kaon decays, this report.